NUMERICAL INVESTIGATION OF LOCALISED FORCED IGNITION OF QUIESCENT GLOBALLY STOICHIOMETRIC STRATIFIED MIXTURES

M. Mehta*, S.P. Malkeson* and N. Chakraborty*

n.chakraborty@liverpool.ac.uk

* School of Engineering, University of Liverpool
Liverpool, L69 3GH, United Kingdom

Abstract

The localised forced ignition of stratified mixtures in a quiescent environment has been studied using three-dimensional numerical simulations where a single step Arrhenius type reaction is used to represent the chemical mechanism. The heat of reaction and the activation energy of the chemical mechanism are taken to be functions of equivalence ratio ϕ in such a manner that a realistic unstrained planar laminar burning velocity $S_{b(\phi)}$ variation with equivalence ratio ϕ representing hydrocarbon-air combustion can be obtained. A pseudo-spectral method is used to initialise the equivalence ratio variation following a bi-modal distribution for prescribed values of global mean $<\phi>$, root-mean-square fluctuation ϕ' and the length scale l_ϕ of equivalence ratio variation. The localised ignition is accounted for by a source term in the energy transport equation which deposits energy for a stipulated time interval. In the present study localised ignition of globally stoichiometric stratified mixtures (i.e. $<\phi>=1.0$) has been studied for different initial values of root-mean-square equivalence ratios (i.e. $\phi'=0.2$, 0.4 and 0.6) and the Taylor micro-scale l_ϕ of ϕ variation (i.e. $l_\phi/l_f=2.7$, 5.6 and 8.2 with l_f being the Zel'dovich flame thickness for stoichiometric mixture). It has been demonstrated that the initial values of ϕ' and l_ϕ/l_f have significant effects on the overall burning rate of the inhomogeneous mixture following localised ignition.

Introduction

Localised ignition of stratified mixtures has applications ranging from Gasoline Direct Injection (GDI) engines to gas turbine relight in aero-engines. However, localised forced ignition of stratified mixtures and the subsequent burning characteristics have received limited attention in comparison to vast body of literature on ignition of homogeneous reactants [1]. The stochastic nature of localised ignition in the context of ignition probability of non-premixed jet flames have been analysed in detail by a number experimental studies [2-5]. Alvani and Fairweather [6] addressed the localised ignition of non-premixed jet flames using Reynolds Averaged Navier Stokes (RANS) simulations. Rashkovosky [7] investigated the effects of spark location with respect to the mixing layer on the spark ignition of laminar inhomogeneous mixtures based on analytical studies. Different aspects of localied ignition of inhomogeneous mixtures under unsteady laminar conditions have analysed using two-dimensional simulations [8-11]. Chakraborty *et al*. [12] and Chakraborty and Mastorakos [13]

studied the effects of turbulence on the localised forced ignition of inhomogeneous mixtures and the influences of the value of mixture fraction ξ and the magnitude of its gradient $|\nabla \xi|$ at the ignitor location on the success and subsequent self-sustained combustion behaviour using three-dimensional Direct Numerical Simulations (DNS) with simplified chemistry. All the aforementioned numerical studies on localised forced ignition of inhomogeneous mixtures [8-13] have been carried for a distribution where the mixture inhomogeneity is characterised by a mean variation of equivalence ratio ϕ with zero root-mean-square (rms) equivalence ratio fluctuation ϕ'. However, the localised ignition of stratified mixtures for a given value of global mean value of equivalence ratio $<\phi>$ but with a non-zero rms equivalence ratio fluctuation ϕ' is yet to be analysed in detail. In the current study, three-dimensional compressible unsteady laminar simulations have been carried out in a quiescent environment. For the purpose of computational economy, a single-step irreversible Arrhenius type chemical reaction has been considered in which the activation energy and the adiabatic flame temperature are taken to be functions of equivalence ratio following the suggestion of Tarrazo *et al*. [14] in such a manner that the laminar burning velocity variation $S_{b(\phi)}$ with equivalence ratio ϕ mimics the realistic equivalence ratio ϕ dependence of the unstrained laminar burning velocity $S_{b(\phi)}$ of typical hydrocarbon flames. In the current study, globally stoichiometric (i.e. $<\phi>=1.0$) mixtures have been considered. The equivalence ratio ϕ variation is initialised using a pseudo-spectral method proposed by Eswaran and Pope [15] which produces a random distribution of ϕ following a bi-modal distribution for specified values of the mean global equivalence ratio $<\phi>$, the rms fluctuation of equivalence ratio ϕ' and the Taylor micro scale of the equivalence ratio variation $l_\phi = \sqrt{6}<[\phi-<\phi>]^2>/<\nabla[\phi-<\phi>].\nabla[\phi-<\phi>]>$ where the angled bracket indicate global mean evaluated over the whole of computational domain. The same approach of initialising the ϕ variation was followed for DNS simulations of turbulent stratified flames in the past [16]. In the current study, values of $\phi' = 0.2,\ 0.4$ and 0.6, and $l_\phi / l_f = 2.7,\ 5.5$ and 8.2 (where $l_f = D_0 / S_{b(\phi=1)}$ is a characteristic chemical length scale where D_0 is the mass diffusivity in the unburned reactants and $S_{b(\phi=1)}$ is the laminar burning velocity of a stoichiometric mixture) have been considered. The main objectives of the current study are to investigate and explain the effects of ϕ' and l_ϕ on the localised forced ignition and on the overall burning characteristics of globally stoichiometric stratified mixtures in the case of successful ignition. Although combustion takes place in a turbulent environment in practical engineering applications, often unsteady laminar simulations play a key role in fundamental understanding of the localised ignition behaviour as done in several previous studies [8-11] and the same approach has been followed here.

Mathematical background

In the present study, the chemical mechanism is simplified by a single-step Arrhenius type chemical reaction representative of hydrocarbon combustion, which takes the following form:

$$Fuel + s.Oxidiser \rightarrow (1+s).Products \qquad (1)$$

where *s* indicates the mass of oxidiser consumed per unit mass of fuel consumption under stoichiometric conditions. The fuel reaction rate is given by an Arrhenius type expression:

$$\dot{w}_F = -\rho B^* Y_F Y_O \exp[-\beta(1-T)/[1-\alpha(1-T)]] \qquad (2)$$

where Y_F and Y_O are the local fuel and oxidiser mass fractions respectively, ρ is the gas density and T is the non-dimensional temperature which is defined as: $T = (\hat{T} - T_0)/(T_{ad(\phi=1)} - T_0)$ where $\hat{T}$ is the instantaneous dimensional temperature, T_0 is the initial reactant temperature and $T_{ad(\phi=1)}$ is the adiabatic flame temperature for the stoichiometric (i.e. $\phi = 1.0$) mixture. In Eq. 2, β is the Zel'dovich number, α is the heat release parameter and B^* is related to the pre-exponential factor,which are defined as:

$$\beta = E_a(T_{ad(\phi=1)} - T_0)/R^0 T_{ad(\phi=1)}^2; \alpha = \tau/(1+\tau) = (T_{ad(\phi=1)} - T_0)/T_{ad(\phi=1)}; B^* = B\exp(-\beta/\alpha) \quad (3)$$

where E_a is the activation energy, R^0 is the universal gas constant, B is the pre-exponential factor and τ is the heat release parameter given by $\tau = (T_{ad(\phi=1)} - T_0)/T_0$. The activation energy E_a and the heat of combustion are taken to be functions of equivalence ratio ϕ according to the suggestion of Tarrazo *et al*. [14]. In the current study, transport quantities including viscosity μ, thermal conductivity λ and the density-weighted mass diffusivity ρD are taken to be equal for all species and independent of temperature. The Lewis numbers of all species are taken to be equal to unity. The combustion is assumed to be taking place in the gaseous phase where all species are perfect gases, which leads to the following state relations: $E = C_V\hat{T} + u_k u_k/2$ and $P = \rho\overline{R}\hat{T}$ where E is the stagnation internal energy, P is the pressure and $\overline{R}$ is the gas constant. Standard values are taken for the ratio of specific heats ($\gamma = C_P/C_V = 1.4$) and Prandtl number ($\mathrm{Pr} = \mu C_P/\lambda = 0.7$). In the combustion of stratified mixtures the species field is often characterised in terms of both passive (i.e. mixture fraction ξ) and active (i.e. fuel mass fraction Y_F) scalars. The mixture fraction ξ can be expressed in terms of both fuel and oxidiser mass fractions in the following manner: $\xi = (Y_F - Y_O/s + Y_{O\infty}/s)/(Y_{F\infty} + Y_{O\infty}/s)$ where $Y_{F\infty}$ is the fuel mass fraction in the pure fuel stream and $Y_{O\infty}$ is the oxidiser mass fraction in air. In the current study, the values for s, $Y_{F\infty}$ and $Y_{O\infty}$ are taken to be: $s = 4$; $Y_{F\infty} = 1.0$ and $Y_{O\infty} = 0.233$.Under these conditions, the stoichiometric fuel mass fraction and stoichiometric mixture fraction values are given by $Y_{Fst} = 0.055$ and $\xi_{st} = 0.055$, respectively. These values are representative of methane/air combustion. The equivalence ratio ϕ can be expressed in terms of ξ and ξ_{st} as $\phi = (1-\xi_{st})\xi/(1-\xi)\xi_{st}$. In the context of stratified combustion, the extent of the completion of the chemical reaction can be characterised by a reaction progress variable, c, which can be defined in terms of the fuel mass fraction Y_F in the following manner as [12,13,16]:

$$c = (\xi Y_{F\infty} - Y_F)/(\xi Y_{F\infty} - \max[0,(\xi - \xi_{st})/(1-\xi_{st})]Y_{F\infty}) \quad (3)$$

According to the above definition, the reaction progress variable c rises monotonically from zero in the fully unburned reactants to unity in the fully burned products. In the current study, the forced ignition due to the heat addition by the ignitor over an energy deposition time is accounted for by including a source term q''' in the energy transport equation [12,13]. The source term q''' is assumed to follow a Gaussian distribution in the radial direction away from the centre of the ignitor [12,13] and is given by in the following manner:

$$q'''(r) = A_q.\exp(-r^2/2R^2) \quad (4)$$

where r is the radial direction from the centre of the ignitor and R is the width of the Gaussian profile [12,13], which is taken to be $R = 1.1l_f$. This choice of R allows for the

sufficient resolution of the temperature gradient and guarantees the rapid disappearance of any artificial effects introduced by the ignition source [12,13]. In Eq. 4, the constant A_q is determined by a volume integration in the following manner:

$$\dot{Q} = \int_V q''' dV \tag{5}$$

where $\dot{Q}$ is the spark power, which is defined in the following manner [12,13]:

$$\dot{Q} = a_{sp}\rho_0 C_P \tau T_0 (4\pi l_f^3/3)[H(t-t_1) - H(t-t_2)]/(t_2 - t_1) \tag{6}$$

where a_{sp} is a parameter that determines the total energy deposited by the ignitor and is taken to be $a_{sp} = 3.6$ in the current study. In Eq. 6, the time instants t_1 and t_2 determine the duration t_{sp} over which the energy is deposited by the ignitor, which is expressed as: $t_{sp} = (t_2 - t_1) = b_{sp} t_f$ where b_{sp} is duration parameter and t_f is a characteristic chemical time scale given by $t_f = l_f / S_{b(\phi=1)}$. In the present study, the value $b_{sp} = 0.2$, which is consistent with the optimum spark duration of $0.2 \le b_{sp} \le 0.4$ indicated by Ballal and Lefebvre [17].

Numerical implementation

A compressible three-dimensional DNS code called SENGA [12,13] was used to carry out the simulations. The initial equivalence ratio distribution is characterised by a random bi-modal distribution of equivalence ratio following the methodology of Eswaran and Pope [15]. In the current study, a stoichiometric global mean equivalence ratio (i.e. $<\phi>=1.0$) has been considered. The initial values of the global mean equivalence ratio $<\phi>$, rms fluctuations of equivalence ratio ϕ', the ratio of Taylor micro-scale of mixture inhomogeneity to the characteristic chemical length scale l_ϕ / l_f are listed in Table 1. In the current study a heat release parameter of $\tau = 3.0$ has been considered in all the cases. The flame Mach number $Ma = S_{b(\phi=1)} / \sqrt{\gamma R T_0}$ for all the cases is taken to be 0.014 and the Zel'dovich number β is taken to be $\beta = 6f(\phi)$ where $f(\phi)$ is a function of equivalence ratio which is given by $1 + 8.25(\phi - 1)^2$ for $\phi \le 0.64$ and $1 + 1.443(\phi - 1.07)^2$ for $\phi \ge 1.07$ according to Tarrazo *et al.* [14]. The value of the function $f(\phi)$ remains unity (i.e. $f(\phi) = 1$) for the equivalence ratio range $0.64 < \phi < 1.07$. The heat release per unit mass of fuel $H_\phi = (T_{ad(\phi)} - T_0) C_P / Y_{F0(\phi)}$ is given by: $H_\phi / H_{\phi=1} = 1$ for $\phi \le 1$ and $H_\phi / H_{\phi=1} = 1 - \alpha_H(\phi - 1)$ for $\phi > 1$ where $\alpha_H = 0.21$ and $Y_{F0(\phi)}$ is the fuel mass fraction in the unburned gas [14].

Table 1: List of initial values of $<\phi>$, ϕ' and l_ϕ / l_f for the cases in the current study.

Case	A	B	C	D	E	F	G	H	I	J
$<\phi>$	1.0	1.0	1.0	1.0	1.0	1.0	1.0	1.0	1.0	1.0
ϕ'	0.0	0.2	0.2	0.2	0.4	0.4	0.4	0.6	0.6	0.6
l_ϕ / l_f	-	2.7	5.5	8.2	2.7	5.5	8.2	2.7	5.5	8.2

The simulation domain is taken to be a cube of the size $21l_f \times 21l_f \times 21l_f$ and the simulation domain is discretised by a Cartesian grid of size $128 \times 128 \times 128$ with uniform grid spacing Δx. The boundaries in the x_1 direction are taken to be partially non-reflecting in nature and are specified using the Navier-Stokes Characteristic Boundary Conditions technique, whereas the boundaries in the other directions are considered to be periodic. A 10th

order central difference scheme was used for spatial differentiation for internal grid pints which gradually reduces to an one-sided 2nd order scheme at non-periodic boundaries. The time advancement is carried out using a third order low-storage Runge-Kutta scheme. For the present study the simulations were carried out for a simulation time of about $8.40t_{sp}$.

Results and Discussion

The temporal evolution of the maximum values of non-dimensional temperature (i.e. $T_{\max}$) and the normalised fuel reaction rate magnitude (i.e. $|\dot{w}_F|_{\max} \times l_f / \rho_0 S_{b(\phi=1)}$) for all the cases are shown in Figs. 1a and b. It can be seen that the temperature rises with time due to energy deposition for $t < t_{sp}$ and the thermal runaway ensues when $T_{\max}$ attains a value close to Zel'dovich temperature $T_c \approx 1 - 1/\beta_{\phi=1}$ and at this point both $T_{\max}$ and $|\dot{w}_F|_{\max} \times l_f / \rho_0 S_{b(\phi=1)}$ increase rapidly with time and this trend continues till $t = 1.0t_{sp}$ as the heat release due to chemical reaction is assisted by the external energy deposition. After $t = 1.0t_{sp}$ the energy deposition is switched off, and the high thermal gradient between the hot gas kernel and the surrounding unburned gas gives rise to higher rate of heat transfer than the rate of heat release. This, in turn, leads to a decrease in $T_{\max}$ and $|\dot{w}_F|_{\max} \times l_f / \rho_0 S_{b(\phi=1)}$ with time. After a long time following energy deposition period the value of $T_{\max}$ approaches to the adiabatic flame temperature of the stoichiometric mixture (i.e. $T \approx 1.0$) and the value of $|\dot{w}_F|_{\max} \times l_f / \rho_0 S_{b(\phi=1)}$ settles to a much smaller value, which no longer changes appreciably with time. The temporal variations of $T_{\max}$ and $|\dot{w}_F|_{\max} \times l_f / \rho_0 S_{b(\phi=1)}$ are found to be consistent with previous numerical studies on localised ignition of inhomogeneous mixtures [12,13].

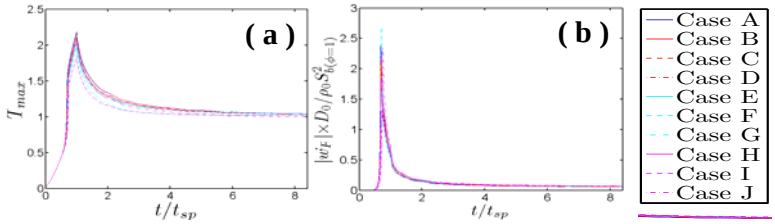

Figure 1 Temporal evolution of (a) $T_{\max}$, and (b) $(\dot{w}_F)_{\max} \times l_f / \rho_0 S_{b(\phi=1)}$ for cases A-J.

The distributions of non-dimensional temperature (T), fuel mass fraction (Y_F), the magnitude of fuel consumption rate ($|\dot{w}_F| \times l_f / \rho_0 S_{b(\phi=1)}$) and the equivalence ratio (ϕ) for cases D, G and J at the central x_1-x_2 plane are shown in Fig. 2 at times $t = 1.0t_{sp}$ and $t = 8.40t_{sp}$ in order to demonstrate the effects of ϕ' for a given value of l_ϕ / l_f. It is important to see that the temperature contours are circular during the period of energy deposition but they become increasingly asymmetrical as time progresses. Before the initiation of combustion the propagation of temperature contours is principally determined by the diffusion of deposited energy, whereas after ignition is initiated, the propagation of isotherms will depend on the magnitude of reaction rate at the local equivalence ratio. It is clear from Fig. 2 that the level of non-uniformity in ϕ distribution decreases as time progresses. Moreover, it can be seen from Fig. 2 that fuel mass fraction Y_F is depleted at the zones associated with high values of T due to consumption of fuel as a result of chemical reaction. It is also evident from Fig. 2 that the volume of burned gas decreases with increasing ϕ'. In

order to understand the effects on l_ϕ / l_f for a given value of ϕ' the temporal evolution of T, Y_F, $|\dot{w}_F| \times l_f / \rho_0 S_{b(\phi=1)}$ and ϕ for cases H, I and J at the central x_1-x_2 plane are shown in Fig. 3. Although the distributions of T, Y_F, $|\dot{w}_F|$ and ϕ for cases H, I and J (shown in Fig. 3) at times $t = 1.0 t_{sp}$ and $t = 8.40 t_{sp}$ are qualitatively similar to the trends demonstrated in Fig. 2, the decay of the mixture inhomogeneity is the quickest in case H and the slowest in case J. At time $t = 8.40 t_{sp}$ the mixture becomes almost homogeneous in case H whereas significant level of equivalence ratio variation survives in cases I and J. It is also evident from Fig. 3 that the volume of burned gas remains comparable for cases H and J, whereas the volume of burned gas is found to be the smallest in case I among cases H, I and J.

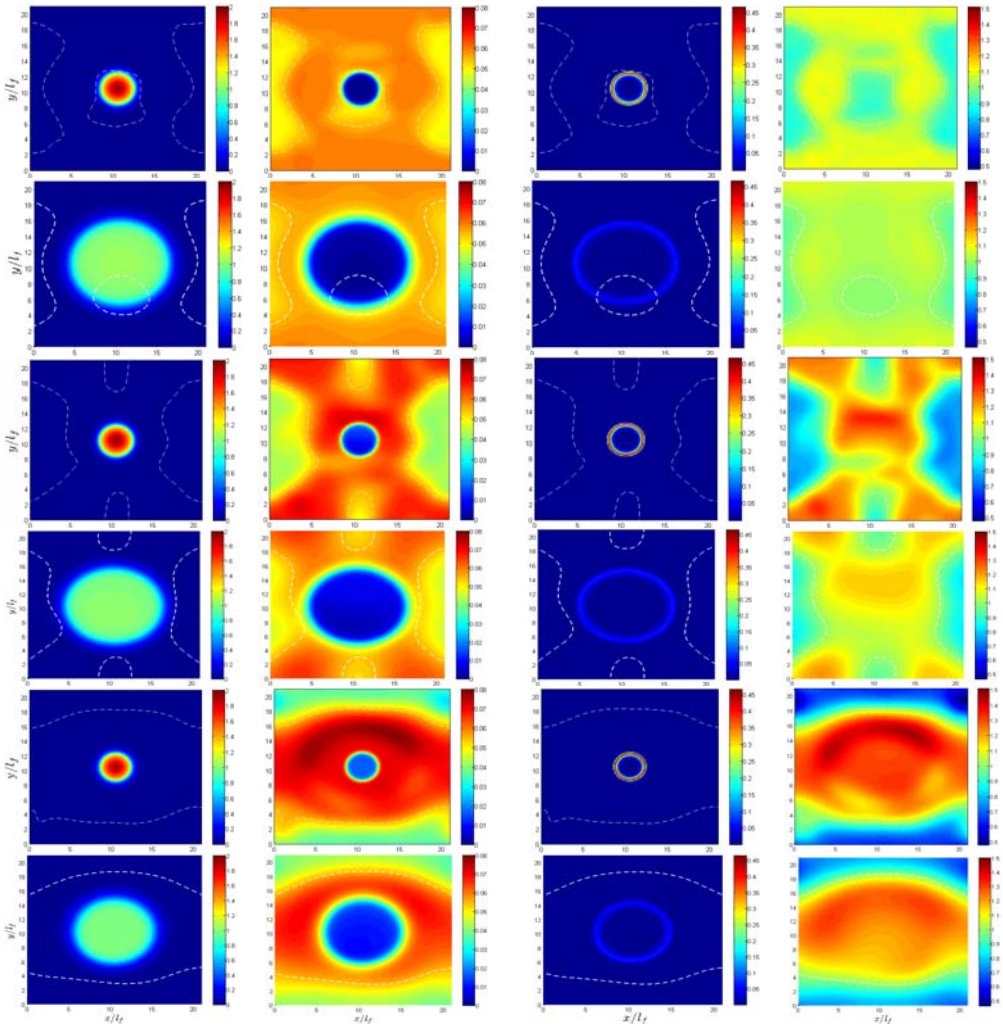

Figure 2 The distributions of T [Column 1], Y_F [Column 2], $\dot{w}_F \times l_f / \rho_0 S_{b(\phi=1)}$ [Column 3] and ϕ [Column 4] at $t = 1.0 t_{sp}$, $8.40 t_{sp}$ [Rows 1-2 for case D], [Rows 3-4 for case G] and [Rows 5-6 for case J] at the central x_1-x_2 plane. The white line indicates the $\xi = \xi_{st}$ contour.

In the combustion of stratified mixtures, the flame index $I_c = \nabla Y_F . \nabla Y_0 / |\nabla Y_F \| \nabla Y_0|$ characterises the mode of combustion which attains positive values for premixed combustion $(I_c > 0)$ and negative values for non-premixed combustion $(I_c < 0)$ [12,13,16]. The

distributions of I_c at the central x_1-x_2 plane for cases D, G, H, I and J at times $t = 1.0t_{sp}$, $t = 4.20t_{sp}$ and $t = 8.40t_{sp}$ are shown in Fig. 4.

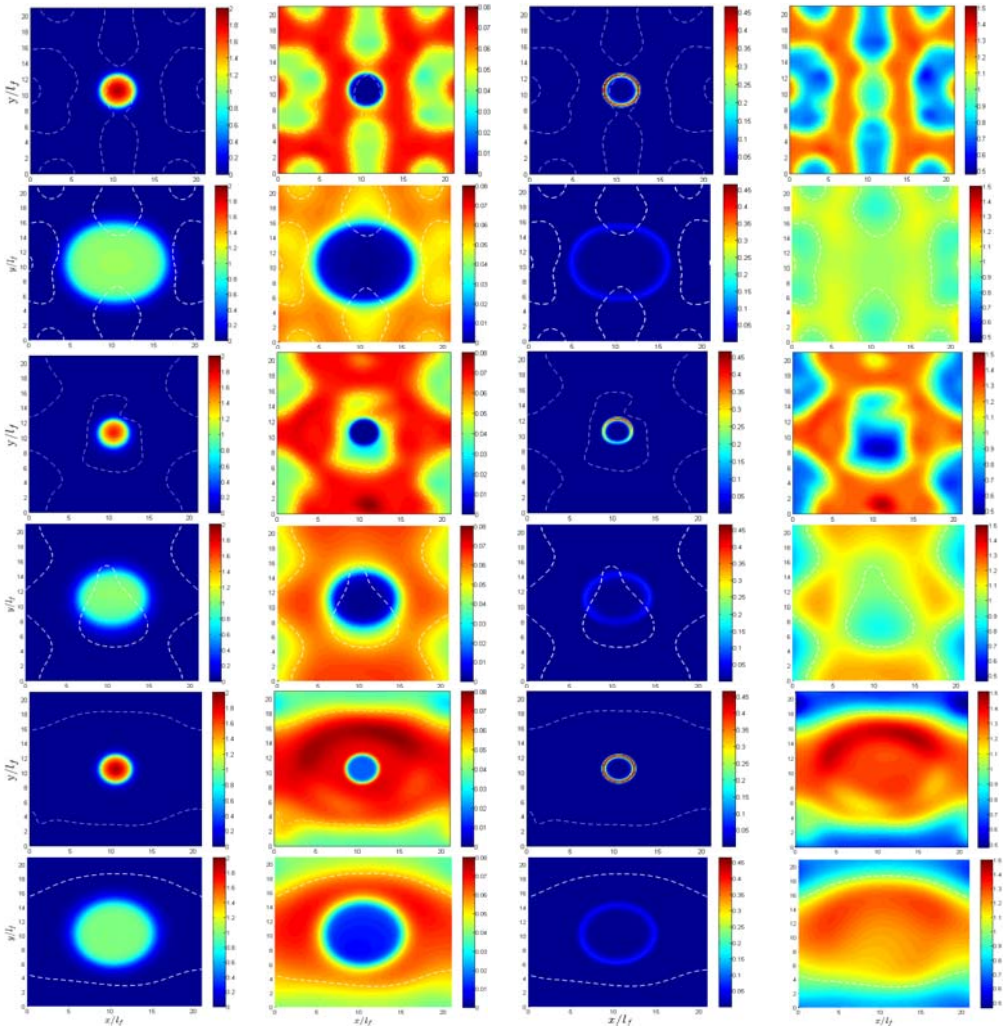

Figure 3 The distributions of T [Column 1], Y_F [Column 2], $\dot{w}_F \times l_f / \rho_0 S_{b(\phi=1)}$ [Column 3] and the equivalence ratio (ϕ) [Column 4] at $t = 1.0t_{sp}$, $8.40t_{sp}$ [Rows 1-2 for case H], [Rows 3-4 for case I] and [Rows 5-6 for case J] at the central x_1-x_2 plane. The white line indicates the $\xi = \xi_{st}$ contour.

Figure 4 reveals that the reaction takes place predominantly in premixed mode (i.e. $I_c > 0$) but localised pockets of $I_c < 0$ are also evident in cases H, I and J indicating the existence of non-premixed combustion. By contrast, in case D the flame index I_c predominantly assumes positive values and the probability of finding negative value of I_c increases with increasing ϕ' for a given value of l_ϕ / l_f because the extent of non-premixed combustion is expected to increase with increasing level of mixture inhomogeneity. Comparing cases H, I and J reveals that the probability of finding $I_c < 0$ decreases with decreasing l_ϕ / l_f for a given value of ϕ'. For all cases the probability of finding $I_c < 0$ decreases as time progresses because of the decrease in the mixture inhomogeneity level. This behaviour can be illustrated by the

temporal evolution of the probability density functions (pdfs) of ϕ of cases D,G, H, I and J, which are shown in Fig. 5. Figure 5 show that although ϕ variation in the simulation domain was initialised as a bi-modal distribution, the width of the pdf decreases with time and the distribution tends towards a Gaussian distribution with a peak at the global mean value of equivalence ratio $<\phi>$ as time progresses. This behaviour of ϕ pdfs arises due to the mixing which acts to reduce the variation of ϕ and produces a Gaussian distribution as the time progresses. It can be seen from Fig. 5 that the effects of mixing are stronger for smaller values of l_ϕ / l.

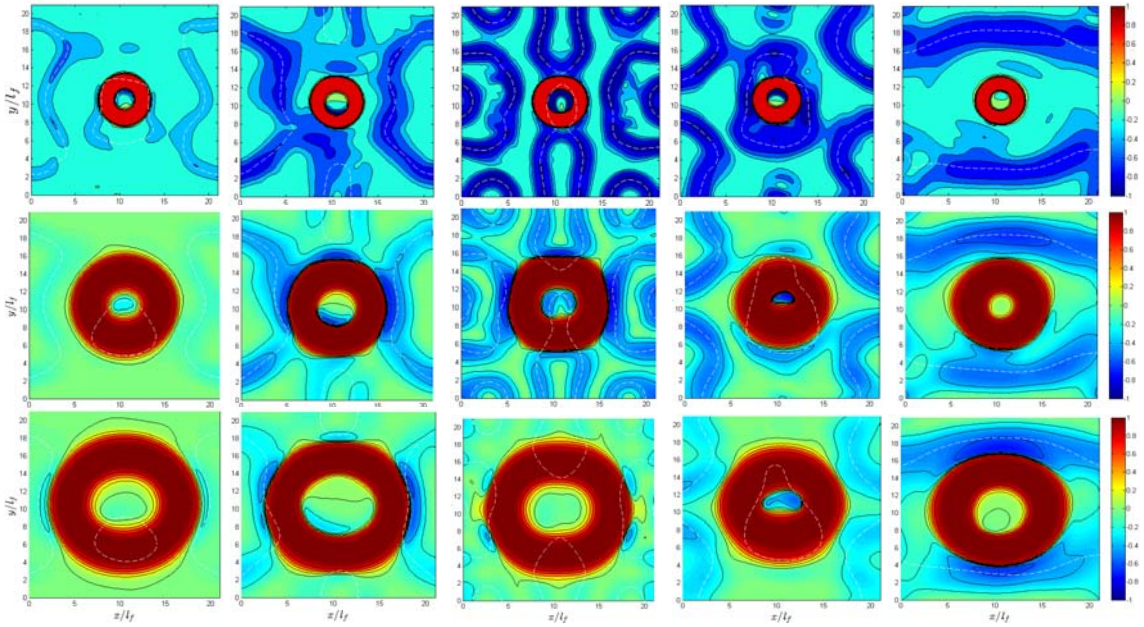

Figure 4 The distributions of $I_c = \nabla Y_F . \nabla Y_0 / \left|\nabla Y_F\right|\left|\nabla Y_0\right|$ at the central x_1-x_2 plane for cases D [Column 1], G [Column 2], H [Column 3], I [Column 4] and J [Column 5] at times $t = 1.0 t_{sp}$ [Row 1], $t = 4.20 t_{sp}$ [Row 2] and $t = 8.40 t_{sp}$ [Row 3].

In order to explain the above behaviour it will be worth presenting the transport equation of ξ''^2 for laminar condition:

$$\rho[\partial \xi''^2 / \partial t + \vec{u}.\nabla \xi''^2] = \nabla.(\rho D \nabla \xi''^2) - 2\rho D \nabla \xi''.\nabla \xi'' \qquad (7)$$

where ξ'' represents the fluctuation of mixture fraction about its global mean value. The terms on the left hand side of Eq. 7 are the transient and advection terms respectively, whereas the first term on right hand side of Eq. 7 denotes molecular diffusion of ξ''^2 and the last term on the right hand side $\rho N_\xi = 2\rho D \nabla \xi''.\nabla \xi''$ acts as a sink and dissipates the fluctuations of mixture fraction. For quiescent laminar flow the term advection term $\rho \vec{u}.\nabla \xi''^2$ remains negligible and the temporal evolution of ξ''^2 (i.e. $\partial \xi''^2 / \partial t$) is primarily driven by the term related to the scalar dissipation rate (i.e. $-2\rho D \nabla \xi''.\nabla \xi''$) along with the molecular diffusion mechanism (i.e. $\nabla.(\rho D \nabla \xi''^2)$). As $N_\xi = 2D \nabla \xi''.\nabla \xi''$ scales as $N_\xi \sim D\xi''^2 / l_\phi^2$ the dissipation rate of ξ''^2 increases with decreasing value of l_ϕ for a given value ϕ' and this suggests that the initial value of dissipation rate is the highest (smallest) in case H (case J) among cases H, I and J and thus the effects of mixing are most (least) prominent in case H (case J) as evident from Fig. 5. These aforementioned behaviours can be substantiated from

the temporal evolution of the rms value of equivalence ratio variation ϕ' evaluated over the whole domain, as presented in Fig. 6. It can be seen from Fig. 6 that ϕ' decays more rapidly for small values of l_ϕ / l_f because of higher value of N_ξ.

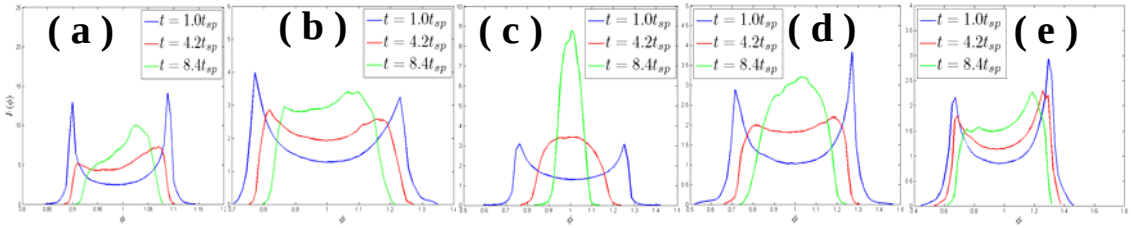

Figure 5 Temporal evolution of the PDFs of equivalence ratio ϕ at $t = 1.0t_{sp}$, $t = 4.20t_{sp}$ and $t = 8.40t_{sp}$ for cases (a) D, (b) G, (c) H, (d) I and (e) J.

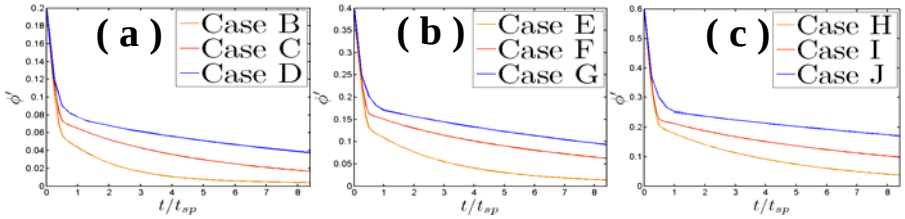

Figure 6 Temporal evolution of ϕ' for cases (a) B-D, (b) E-G, and (c) H-J.

The scatter of normalised fuel reaction rate magnitude $|\dot{w}_F| \times l_f / \rho_0 S_{b(\phi=1)}$ with ξ is presented in Fig. 7a at $t = 8.40t_{sp}$ for case G. A considerable amount of temperature variation on mixture fraction isosurfaces is responsible for the large scatter of $|\dot{w}_F| \times l_f / \rho_0 S_{b(\phi=1)}$ in Fig. 7a. It is evident that from Fig. 7a that the maximum reaction rate in case G is attained towards the slightly rich side (i.e. $\xi \approx 0.06$) which corresponds to $\phi \approx 1.10$ where the unstrained planar laminar burning velocity $S_{b(\phi=1)}$ attains its maximum value. The temporal evolution of the mean values of $|\dot{w}_F| \times l_f / \rho_0 S_{b(\phi=1)}$ conditional on ξ at different time instants is shown in Fig. 7b, which demonstrate the temperature distribution remains qualitatively similar following successful ignition. The variation of $|\dot{w}_F| \times l_f / \rho_0 S_{b(\phi=1)}$ with reaction progress variable c for case G at $t = 8.0t_{sp}$ is presented in Fig. 7c, which show that the maximum value of $|\dot{w}_F| \times l_f / \rho_0 S_{b(\phi=1)}$ takes place close to $c = 0.8$, which is consistent with reaction rate profiles of perfectly-premixed flames in the context of simplified chemistry [12,13]. The reaction rate scatter with c arises due to the equivalence ratio variation on a given c isosurface in the present configuration. In addition to the variation of the equivalence ratio, the mixture fraction gradient also significantly affects the reaction zone structure [12,13]. The effects of the mixture fraction gradient can be characterised by the density-weighted scalar dissipation rate $\chi_\xi = \rho D \nabla \xi . \nabla \xi / \rho_0$. The variation of the magnitude of the normalised fuel reaction rate $|\dot{w}_F| \times l_f / \rho_0 S_{b(\phi=1)}$ with normalised density-weighted scalar dissipation rate $\chi_\xi t_f / \xi_{st}^2 (1-\xi_{st})^2$ for case G at $t = 8.40t_{sp}$ is shown in Fig. 7d. The variation of mean values of $|\dot{w}_F| \times l_f / \rho_0 S_{b(\phi=1)}$ conditional on scalar dissipation rate values in the reaction progress range $0.7 \le c \le 0.9$ where $|\dot{w}_F| \times l_f / \rho_0 S_{b(\phi=1)}$ assumes high values (see Fig. 7c) is shown in Fig. 7e. It is evident from Fig. 7e that $\dot{w}_F \times l_f / \rho_0 S_{b(\phi=1)}$ is negatively

correlated with $\chi_\xi t_f / \xi_{st}^2 (1-\xi_{st})^2$ at the maximum reaction rate location and high values of $\dot{w}_F \times l_f / \rho_0 S_{b(\phi=1)}$ are associated with small values of $\chi_\xi t_f / \xi_{st}^2 (1-\xi_{st})^2$. This is in agreement with previous findings in the context of autoignition [18] and localised forced ignition [12,13] of inhomogeneous mixtures. The negative correlation between $|\dot{w}_F| \times l_f / \rho_0 S_{b(\phi=1)}$ and $\chi_\xi t_f / \xi_{st}^2 (1-\xi_{st})^2$, which indicates that the reaction rate attains relatively higher values where the combustion is taking place predominantly in premixed mode. Although the variations are shown for case G in Fig. 7, the same qualitative behaviour has been observed for the other stratified cases.

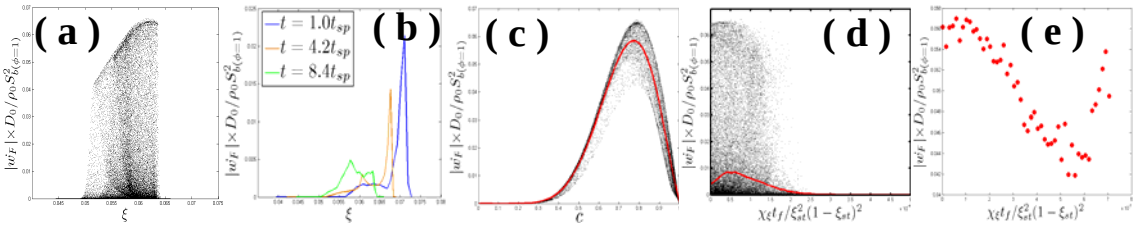

Figure 7 (a) Variation of $|\dot{w}_F| \times l_f / \rho_0 S_{b(\phi=1)}$ with ξ at $t = 8.40t_{sp}$. (b) Variation of $|\dot{w}_F| \times l_f / \rho_0 S_{b(\phi=1)}$ conditional on ξ at $t = 1.0t_{sp}$, $t = 4.20t_{sp}$ and $t = 8.40t_{sp}$. (c) Variation of $|\dot{w}_F| \times l_f / \rho_0 S_{b(\phi=1)}$ with c at $t = 8.40t_{sp}$. (d) Variation of $|\dot{w}_F| \times l_f / \rho_0 S_{b(\phi=1)}$ with $\chi_\xi t_f / \xi_{st}^2 (1-\xi_{st})^2$ at $t = 8.40t_{sp}$. (e) Variation of mean values of $|\dot{w}_F| \times l_f / \rho_0 S_{b(\phi=1)}$ conditional on $\chi_\xi t_f / \xi_{st}^2 (1-\xi_{st})^2$ in the range $0.7 \le c \le 0.9$ at $t = 8.40t_{sp}$. Variations of conditional mean values are shown by red lines in Figs. 7c-e. All the figures are shown for case G.

The extent of burning can be characterised by the volume of burned gas mass m_b with $c \ge 0.9$. The temporal evolutions of the burned gas mass normalised by the mass of unburned gas with a radius equal to l_f (i.e. $4/3\rho_0 \pi l_f^3$) for different values of ϕ' at $l_\phi / l_f = 2.7$, 5.5 and 8.2 are shown Figs. 8a-c respectively along with the variation of $m_b(c \ge 0.9)/(4/3\rho_0 \pi l_f^3)$ obtained for the premixed case (i.e. case A) for the same value of global mean equivalence ratio $<\phi>$. It can be observed from Figs. 8a-c that an increase in ϕ' leads to a decrease in the burned gas mass. The burning rate of mixtures with $\phi < 1.0$ and $\phi \ge 1.10$ is smaller than that in the stoichiometric mixture (i.e. $\phi = 1.0$) and as a result of this the extent of burning is smaller in the stratified mixtures than the homogeneous mixture with $\phi = 1.0$. The probability of finding $\phi < 1.0$ and $\phi \ge 1.10$ increases with increasing ϕ' and this gives rise to reduction in burning rate for higher value of ϕ'. The temporal variations of $m_b(c \ge 0.9)/(4/3\rho_0 \pi l_f^3)$ shown in Figs. 8a-c are replotted in Figs. 8d-f for $\phi' = 0.2$, 0.4 and 0.6 respectively to illustrate the effects of l_ϕ / l_f. It can be seen from Figs. 8d-f that the smallest extent of burning is obtained for $l_\phi / l_f = 5.5$ for all values of ϕ' considered here, and the extent of burning for $l_\phi / l_f = 2.7$ and 8.2 remain comparable to the extent of burning in the premixed case. It has been demonstrated earlier in Figs. 3, 5 and 6 that the effects of mixing is the strongest for the $l_\phi / l_f = 2.7$ cases and thus the stratified mixture with $l_\phi / l_f = 2.7$ approaches to an almost homogeneous mixture with $<\phi>=1.0$ and thus the extent of burning in the $l_\phi / l_f = 2.7$ case remains comparable to the homogeneous mixture case. The non-zero probability of finding slow-burning mixtures with $\phi < 1.0$ and $\phi \ge 1.10$

even in the $l_\phi / l_f = 2.7$ cases (see Figs. 3, 5 and 6) reduces the burning rate in comparison to the homogeneous mixture with $\phi = 1.0$ .For the high values of l_ϕ / l_f the clouds of non-uniform fuel-air distributions are relatively big and as a result of this there is a high probability of encountering a large region of almost homogenous mixture at the location where the centre of ignitor is located (see Fig. 3). If the ignitor centre is located in the vicinity of a large cloud of $1.0 \le \phi \le 1.1$, as shown in Fig. 3, the slow burning rate in the pockets $\phi < 1.0$ encountered during the expansion of hot gas kernel is mostly compensated by the high burning rate in the mixture with $1.0 \le \phi \le 1.1$ and this leads to the burned gas mass in $l_\phi / l_f = 8.2$ case which is comparable to that obtained in the case of homogeneous mixture (i.e. case A). In the $l_\phi / l_f = 5.5$ case, there is a significant presence of the clouds of non-uniform distributions of fuel-air mixture near the ignitor centre and in the vicinity of the expanding hot gas kernel at all stages. This gives rise to significantly high probabilities of finding slow-burning mixtures corresponding to $\phi < 1.0$ and $\phi \ge 1.10$ in the reaction zone for the $l_\phi / l_f = 5.5$ case, and the smaller rate of burning in the pockets with $\phi < 1.0$ and $\phi \ge 1.10$ leads to a reduced burning rate in comparison to the homogeneous mixture and stratified mixtures with $l_\phi / l_f = 2.7$ and 8.2 (see Figs. 8d-f).

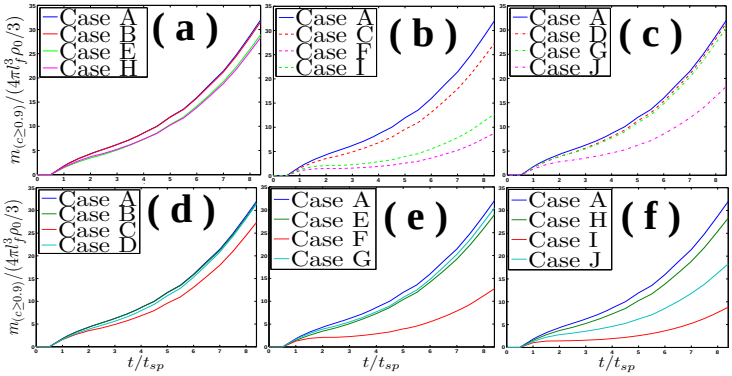

Figure 8 The temporal evolutions of the burned gas mass normalised by the mass of unburned gas with radius equal to l_f (i.e. $4/3\rho_0\pi l_f^3$) $m_b(c \ge 0.9)/(4/3\rho_0\pi l_f^3)$ for cases (a) A, B, E and H, (b) A, C, F and I, (c) A, D, G and J, (d) A-D, (e) A and E-G, and (f) A and H-J.

Conclusions

Localised forced ignition of initially quiescent globally stoichiometric (i.e. $<\phi>=1.0$) stratified mixtures is investigated using three-dimensional simulations for different initial values of rms equivalence ratio variation ϕ' and Taylor micro-scale of equivalence ratio variation l_ϕ. It has been shown that the resulting flame shows predominantly premixed mode of combustion although some localised pockets of non-premixed combustion have been observed for high values of ϕ' and l_ϕ / l_f. It has been demonstrated that the initial values of ϕ' and l_ϕ / l_f have significant influences on the overall burning behaviour. For a given value of l_ϕ / l_f an increase in ϕ' is shown to decrease the extent of burning. The influence of l_ϕ / l_f on the overall extent of burning has been found to be non-monotonic, and the extent of burning for $l_\phi / l_f = 2.7$ and 8.2 remain comparable to that obtained in the case of homogeneous mixture with $\phi = 1.0$, but the extent of burning for $l_\phi / l_f = 5.5$ is smaller than those obtained for the homogeneous mixture and stratified mixtures with $l_\phi / l_f = 2.7$ and 8.2.

Detailed physical explanations have been provided for the observed influences on ϕ' and l_ϕ / l_f on the extent of burning of stratified mixtures following successful localised ignition.

Acknowledgements

SPM and NC gratefully acknowledge the financial assistance of the EPSRC UK.

References

[1] Mastorakos, E., "Ignition of turbulent non-premixed flames", *Prog. Energy Combust*. Sci., **35**, 57-97 (2009).

[2] Birch, A. D. Brown, D.R. Dodson, M.G., Ignition probabilities in turbulent mixing flows, *Proc. Combust. Inst.* **18,** 1775-1780 (1981).

[3] Smith, M. T. E., Birch, A. D., Brown, D. R., Fairweather, M., "Studies of ignition and flame propagation in turbulent jets of natural gas, propane and a gas with high hydrogen content", *Proc. Combust. Inst.* **21**,1403-1408(1986).

[4] Ahmed, S. F., Mastorakos, E., "Spark Ignition of lifted turbulent jet flames", *Combust. Flame*, **146,** 215-231 (2006).

[5] Ahmed, S. F., Balachandran, R., Mastorakos, E., "Measurements of ignition probability in turbulent non-premixed counterflow flames", *Proc. Combust. Inst.*, **31,** 1507-1513 (2007).

[6] Alvani, R.E., Fairweather, M.,Ignition Characteristics of Turbulent Jet Flows, *Trans. Ichem E*, **80**, 917-923 (2002).

[7] Rashkovoksky, S.A., "Spark ignition in imperfectly mixed reactants", *Proc. of 1st Mediterranean Combust. Symp.*, Anatalya, Turkey, pp. 1403-1411 (1999).

[8] Ray, J., Najm, H.N., McCoy, R.B., "Ignition front structure in a methane air jet", Paper no. 150, 2nd Joint Meeting of the U.S. Section of the Combustion Institute, Oakland, California, (2001).

[9] Hilbert, R., Thevenin, D., "DNS of multibrachial structures with detailed chemistry and transport", Paper no. 064, 9th International Conference on Numerical Combustion, Sorrento, Italy (2002).

[10] Im, H.G., Chen, J.H., "Structure and propagation of triple flames in partially premixed hydrogen–air mixtures". *Combust. Flame*, **119**, 436-454, (1999).

[11] Richardson, E. S., Mastorakos, E., "Numerical investigation of spark ignition in a laminar methane-air counterflow", *Combust. Sci. Tech.*, **179** (1-2), 21-37 (2007).

[12] Chakraborty, N., Mastorakos, E., Cant, R.S., "Effects of turbulence on spark ignition in inhomogeneous mixtures: A Direct Numerical Simulation (DNS) study". *Combust. Sci. Tech.*, **179**, 293-317, (2007).

[13] Chakraborty, N., Mastorakos, E., "Direct Numerical Simulations of localised forced ignition in turbulent mixing layers: the effects of mixture fraction and its gradient", *Flow Turb. Combust*., 80,155-186(2008).

[14] Tarrazo, E., Sanchez, A., Linan, A., Williams, F., "A simple one-step chemistry model for partially premixed hydrocarbon combustion". *Combust. Flame*, **147**, 32–38, (2006).

[15] Eswaran, V., Pope, S.B., "Direct numerical simulations of the turbulent mixing of a passive scalar". *Phys. Fluids*, **31**, 506–520, (1988).

[16] Helie, J., Trouve, A., "Turbulent flame propagation in partially premixed combustion", *Proc. Combust. Inst.*, **27**, 891–898, (1998).

[17] Ballal, D.R., Lefebvre, A.: Spark ignition of turbulent flowing gases, presented at the 15th Aerospace Sciences Meeting, AIAA Los Angeles, paper no. 77-185 (1977).

[18] Mastorakos, E., Baritaud, T.A., Poinsot, T. J., "Numerical simulations of autoignition in turbulent mixing flows", *Combust. Flame,* **109,**198-223 (1997).